

ARTICLE / INVESTIGACIÓN

Infrared Imaging of Skin Cancer Cell Treated with Copper Oxide and Silver Nanoparticles

Mazin M. Mowat¹, Majid Shannon Khallaf², and Basaad Hadi Hamza^{1*}

DOI. 10.21931/RB/2023.08.02.51

¹ Department of Physics, College of Sciences, Mustansiriyah University, Iraq.² Materials Directorate, Ministry of Science and Technology, Iraq.

Corresponding author: Bassaadhadi@yahoo.com

Abstract: Copper oxide and silver nanoparticles were used to treat the skin cancer cell with different concentrations, such: (5, 10 and 15ml) at a mixing ratio of 1:1. The characterization of skin cancer lesions pics was taken using a super speed monochrome CMOS camera (Model: ZWO, ASI 120 MM-S). Also, the effect of exposure time on the IR radiation was studied using an IR source connected to this camera. The MTT assay measured cell viability against the control sample cell lines. The results show that both copper oxide and silver nanoparticles appear a high activity against the skin cancer cell line.

Key words: IR imaging, Skin cancer cell, Nanoparticles, MTT assay.

Introduction

Nanomedicine, which combines nanotechnology and medicine, offers several benefits over traditional cancer treatments, including adaptability, effective drug transport, and controlled chemotherapeutic agent release. Nanoparticles have unique physical and chemical qualities, such as small size, chemical composition, huge surface area, customized form, and structure, which allow them to provide these advantages^{1,3}. NPs naturally travel to the spleen and lymph organs, making them attractive candidates for delivering immunotherapeutic drugs, whether polymeric, liposomal, or metallic formulations⁴. Furthermore, nanomaterials can be employed as cytotoxics and/or enhancers of traditional chemotherapies, reducing side effects, increasing blood circulation time, and preventing drug degradation before it reaches the target location⁵. In nanomedicine, silver NPs are a well-studied substance. Biocompatibility, huge surface-to-volume ratio, potent antibacterial activity, and cytotoxicity against cancer cells are just a few of the physicochemical and biological features of Ag NPs⁶. Copper oxide nanoparticles (CONPs) are another nanomaterial with biomedical applications⁷. CuO NPs, specifically, have been shown to have pharmacological effects in tumor therapy, including triggering apoptosis, boosting ROS production, preventing metastasis, and activating autophagic cell death. (8,12), in colon cancer, esophageal cancer, lung cancer, and breast cancer. as well as melanoma¹³. Through thermal infrared cameras, infrared thermal imaging (IRT) can monitor the temperature variations of a specific skin area. This imaging technique can be used actively (dynamic thermography) by applying a cold or hot stimulus to disrupt the thermal balance or passively (static thermography) by acquiring temperature distribution without temperature changes¹⁴. The amount of heat the skin emits heavily depends on peripheral blood flow. This anatomical feature is significantly impacted when a physiological change occurs, such

as the growth of a skin tumor¹⁵. Because malignant tumors have higher metabolic activity than benign lesions, distinct temperature disturbances should be expected for different neoplasia, such as hyperthermic patterns for the first and hypothermic variations for the second This feature, combined with the other advantages of IRT, such as non-invasiveness, contact lessness, low cost, quickness, and non-ionization¹⁶, has prompted writers to investigate the use of IRT for skin cancer diagnosis in recent years¹⁷.

Materials and methods

The Ag and/or CuO NPs (Sigma, Aldrich, 99.9%) were used to detect the anticancer activity of these NPs on the skin cancer cell line. The NPs were diluted as a suspension with three concentrations such: (5, 10, and 15 ml), fixing the mixing ratio of these NPs as (1:1). The characterization of skin cancer lesions images was taken using a super speed monochrome CMOS camera (Model: ZWO, ASI 120 MM-S). Also, the effect of exposure time to the IR radiation was studied by using an IR source connected to this camera. Human skin cancer cell lines squamous cell carcinoma (SCC), SK-MEL-28 (skin melanoma), and MeWo (melanoma lymph node metastasis), as well as standard nontumorigenic skin cell lines [normal immortalized keratinocyte (NIK) and human fibroblast cell (HFC)] were cultured in DMEM supplemented with 10% fetal bovine serum, 100 units of penicillin/ml, and all cells were cultivated at 37°C in a 5% CO₂ atmosphere. In these cells, there was no cross-contamination. The 3-(4,5-Dimethylthiazol-2-yl)-2,5-diphenyltetrazolium bromide (MTT)-dye test was used to examine dose-dependent death of skin cancer and normal cells (17–18). Before adding the PBS vehicle to the culture medium, cells were seeded in 96-well flat-bottom tissue culture plates (Falcon, Becton Dickson Labware, Franklin Lakes, NJ).

Citation: Mowat, M.M.; Khallaf, M.S.; Hamza, B.H. Infrared Imaging of Skin Cancer Cell Treated with Copper Oxide and Silver Nanoparticles. *Revis Bionatura* 2023;8 (2) 51. <http://dx.doi.org/10.21931/RB/2023.08.02.51>

Received: 15 May 2023 / **Accepted:** 10 June 2023 / **Published:** 15 June 2023

Publisher's Note: Bionatura stays neutral with regard to jurisdictional claims in published maps and institutional affiliations.

Copyright: © 2022 by the authors. Submitted for possible open access publication under the terms and conditions of the Creative Commons Attribution (CC BY) license (<https://creativecommons.org/licenses/by/4.0/>).



A conventional MTT-dye test (Sigma) evaluated live cells three days after treatment began. Conditions of the experiment: cells were grown for 24 hours before treatment. At least two experiments were carried out.

Results

A benign skin cell's thermal reaction is identical to that of healthy skin tissue, as opposed to skin cancer cells. As a result, thermographic imaging can identify an increase in the metabolic activity of a skin cancer lesion. The images were configured in the thermographic cameras for the skin cancer cell line, and a measurement range was chosen so that the upper temperatures were close to the usual maximum body temperature, and the wavelengths ranged from 1 to 3 m. This imaging aims to characterize the demographic images of skin cancer cell lines to find a marker for the condition's presence.

The images in the current study have the combination of the three components of the cells called the nucleus (blue), the endoplasm (the cell under consideration and it is red) and the cytoskeleton (green). The nucleus is the cell's control center; the endoplasm is the part where the cell activity occurs and has the nucleus in it. The cytoskeleton is the outer frame or the skeleton of the cell. To kill or to eliminate the cancerous cells, CuO NPs and/or Ag NPs with different concentrations were used, and the images of the cells with defective protein were observed using a fluorescence image microscope and IR camera. The intensity of the cells in the images indicates how the cell's future state will be. In the current situation, the greater intensity in the cells indicates that the cell will die. This also means that the NPs used successfully kill the cancerous cell. As expected, no

detectable cancer signal was observed in the control sample where no red color was observed in this image figure (1- a). Conversely, in figures (1- b), (2- a, b) and (3- a, b), red field observation indicated that cancer cells were viable throughout the imaging study. On the other hand, comparatively weak signals could be observed in the infrared images when the various concentrations of CuO NP's and Ag NP's were added to the cancer cell line.

It is clear from the images shown in Figure 2- a by adding 5ml of CuO NP's suspension into the cell line, there is a weak response, and the cancer cell is still available (the red signals), but when mixing CuO NP's with Ag NP's these signal will reducing obviously and also, increasing the concentration of CuO NP's leads to a decreasing in cancer cell signal as shown in figures (3- a) and (4- a). So, adding CuO NP's and/or Because of their tiny size and the poor tumor vasculature, Ag NPs can selectively collect on tumor tissues, as demonstrated in figures (3 c) and (3 d) (4- c). MIR imaging could distinguish cell lines and be a potential tool for in vivo tumor image analysis in animal models. This would be a critical step toward realizing the ultimate goal of using this dye-free approach for intraoperative surgical procedures. This indicates that MIR characteristics can be used to assess resection margins. Figures 5a, b, c, and d demonstrate IR imaging without nanoparticles and with different IR exposure durations (2, 4, 6, and 8 minutes, respectively).

Figures 6, 7 and 8 show IR imaging by adding Ag NP's suspension with (5, 10 and 15 ml), and figures (6, 7 and 8 b) show the IR image by adding Ag NP's suspension with (5, 10 and 15 ml). In contrast, figures (6, 7 and 8 c) show IR imaging by adding CuO: Ag mixing ratio as (1:1) at the concentration such (as 5, 10, and 15 ml) and with IR exposure

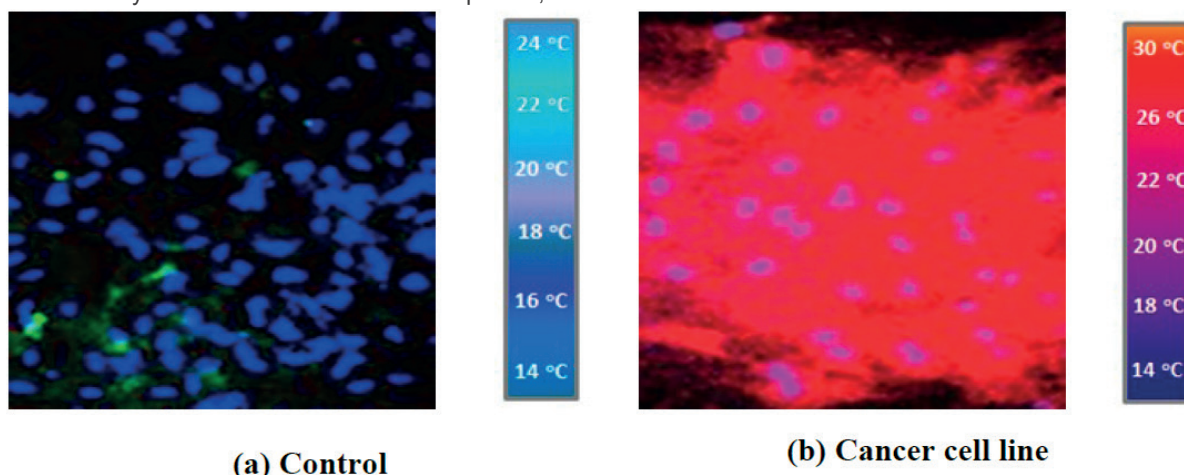


Figure 1. The IR images of the (a) control cell and (b) cancer cell line.

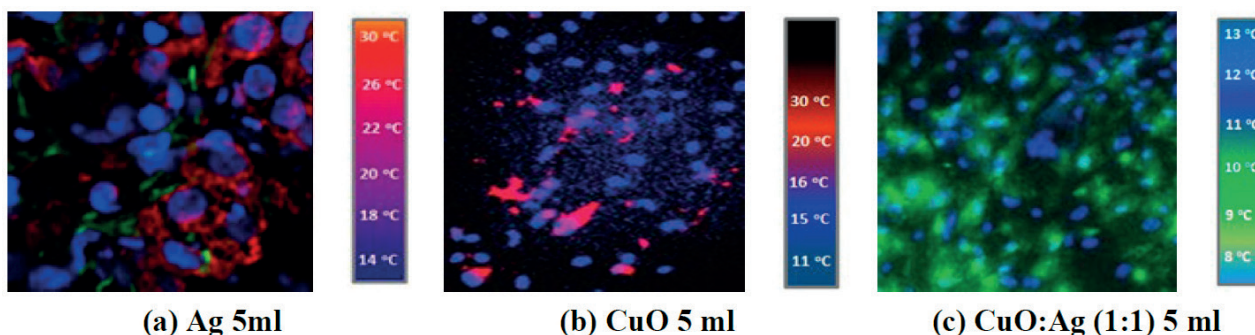
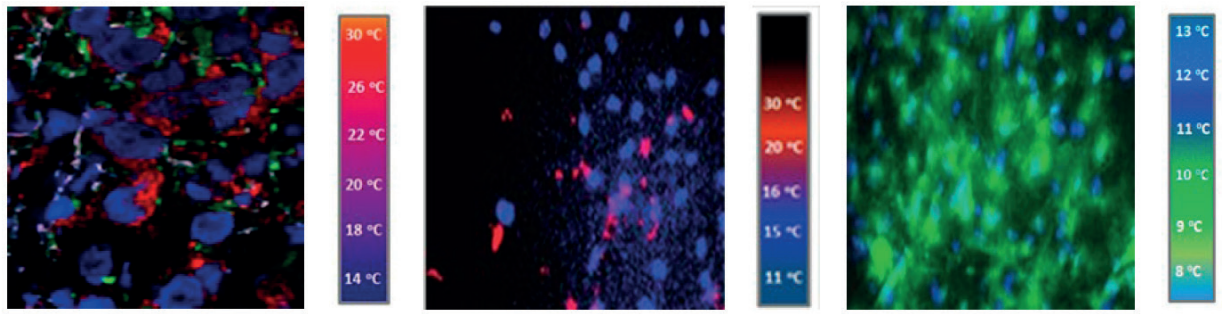


Figure 2. IR images of cancer cell line treated by (a) 5ml of Ag concentration, (b) 5ml of CuO concentration, and (c) 5ml of CuO: Ag concentration with the mixing ratio of 1:1.

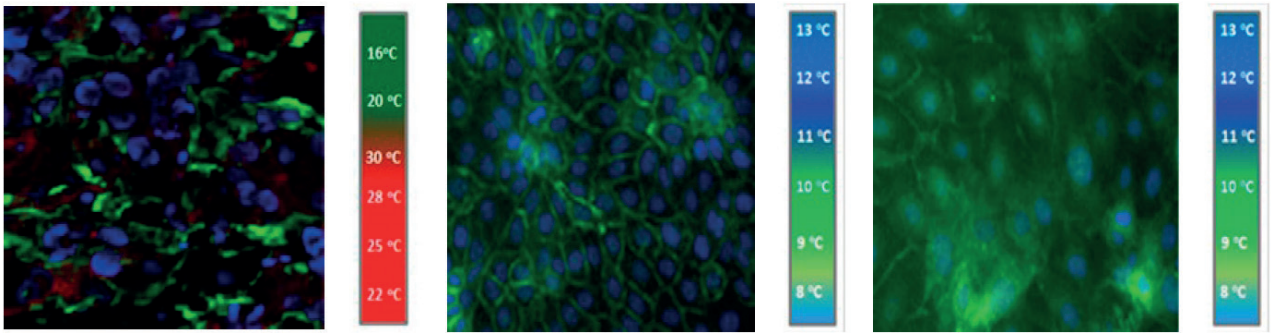


(a) Ag 10ml

(b) CuO 10ml

(c) CuO:Ag (1:1) 10ml

Figure 3. IR imaging of a cancer cell line treated with (a) 10ml Ag, (b) 10ml CuO, and (c) 10ml CuO: Ag with a 1:1 mixing ratio.

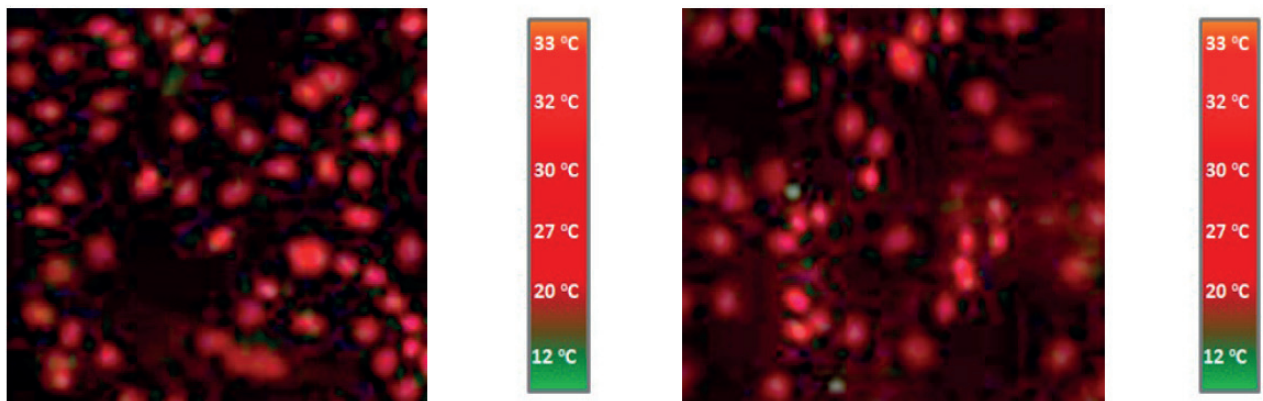


(a) Ag 15ml

(b) CuO 15ml

(c) CuO:Ag (1:1) 15ml

Figure 4. IR pictures of a cancer cell line treated with (a) 15ml of Ag, (b) 15ml of CuO, and (c) 15ml of CuO: Ag concentration with a 1:1 mixing ratio.



(a) 2 min

(b) 4 min

(c) 6 min.

(d) 8 min.

Figure 5. IR imaging with IR exposure at different exposure times (2, 4, 6 and 8 min.), respectively.

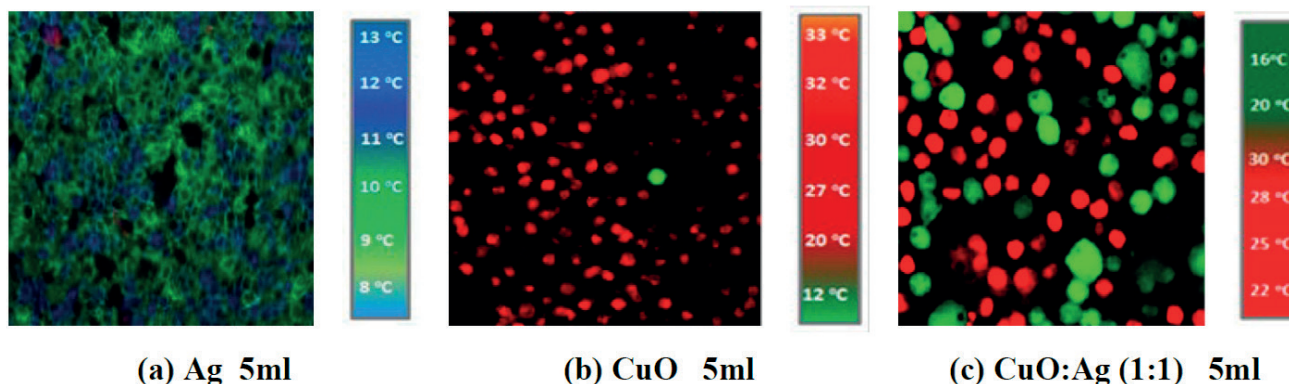


Figure 6. IR images of skin cancer cells with add (a) 5ml of Ag NP's (b) 5ml of CuO NP's suspension, and (c) 5ml of CuO: Ag (1:1) under IR exposure at 8min.

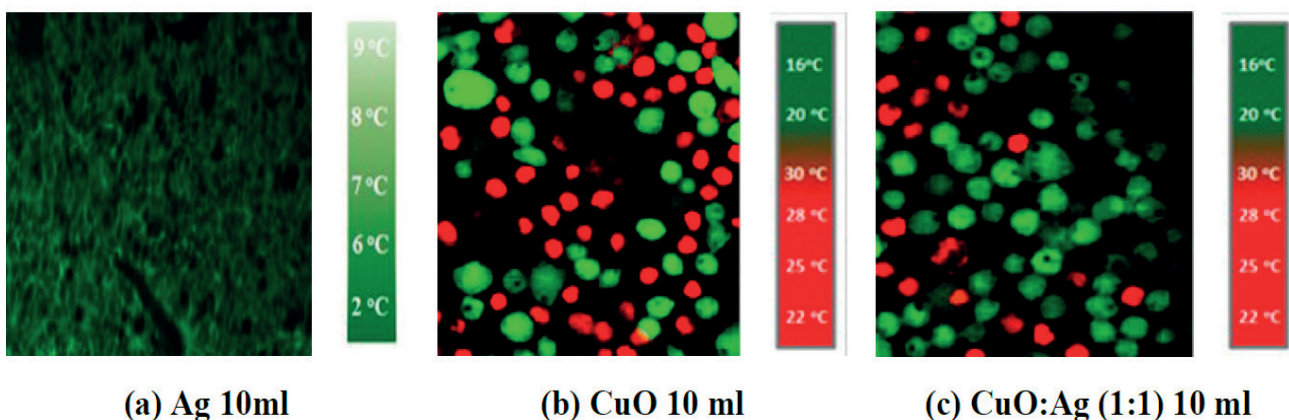


Figure 7. IR images of skin cancer cells with add (a) 10ml of Ag NP's, (b) 10ml of CuO NP's suspension, and (c) 10ml of CuO: Ag (1:1) under IR exposure at 8min.

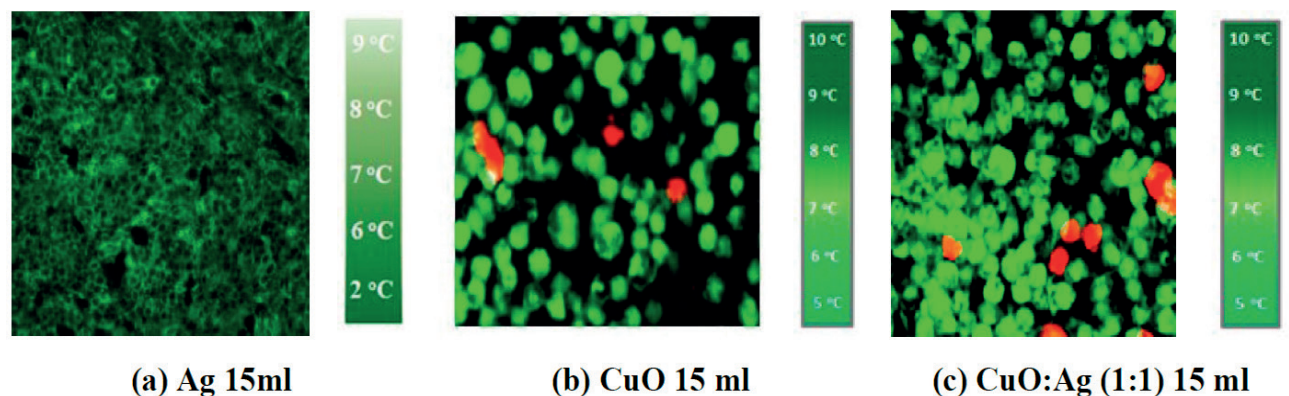


Figure 8. IR images of skin cancer cells with add (a) 15ml of Ag NP's (b) 15ml of CuO NP's suspension, and (c) 15ml of CuO: Ag (1:1) under IR exposure at 8min.

at fixed exposure time as 8min.

Copper oxide nanoparticles significantly reduced the number of skin cancer cells in a dose-dependent manner. Figure (9-a) shows the cell viability with adding only CuO NP's without IR radiation, while figure (9-b) shows the cell viability when adding CuO NP's with IR radiation exposure.

It can be seen that as the concentration of CuO NP was increased, the degree of cell death rose. IR radiation's effect on skin cancer's viability is also visible. Cell viability was less than 50% in both cell lines when treated with 1.6g/ml, as shown in Figure 9-a without IR radiation, indicating the presence of an active CuO NP's agent. However, when treated with 1.6 g/ml and exposed to IR radiation, practically all these NPs showed more than 50% cell survival in both cell lines. As the concentration of CuO NPs increased, the percentage of cell viability dropped, resulting in a negative

association.

Figure 10-a shows the cell viability with adding only Ag NPs without IR radiation, while figure (10-b) shows the cell viability when adding Ag NPs with IR radiation exposure.

At a 1.6 g/ml concentration, the Ag NPs killed 40 percent of skin cancer cells before being exposed to IR radiation.

Figures 11-a and b show the skin cancer cell line viability treated with CuO: Ag NP's with the mixing ratio of (1:1) at different concentrations without and with IR radiation exposure, respectively.

Discussion

From Figures (6-a, 7-a, and 8-a) it is clear that the skin

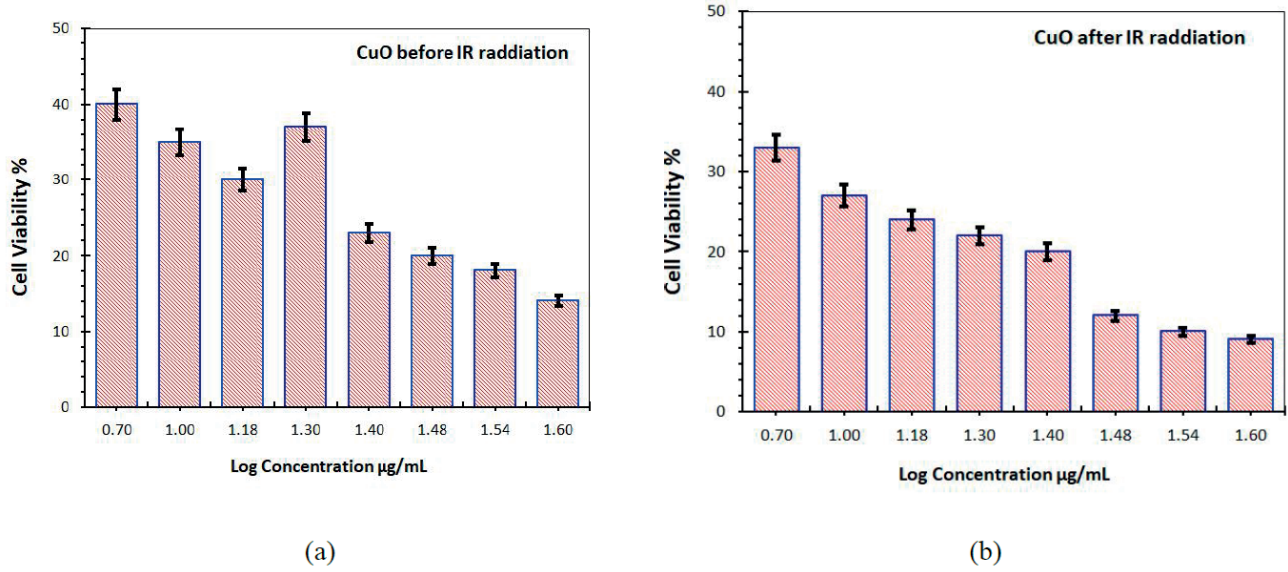


Figure 9. Cell viability of the skin cancer cell treated with CuO NP's (a) without IR radiation (b) with IR radiation.

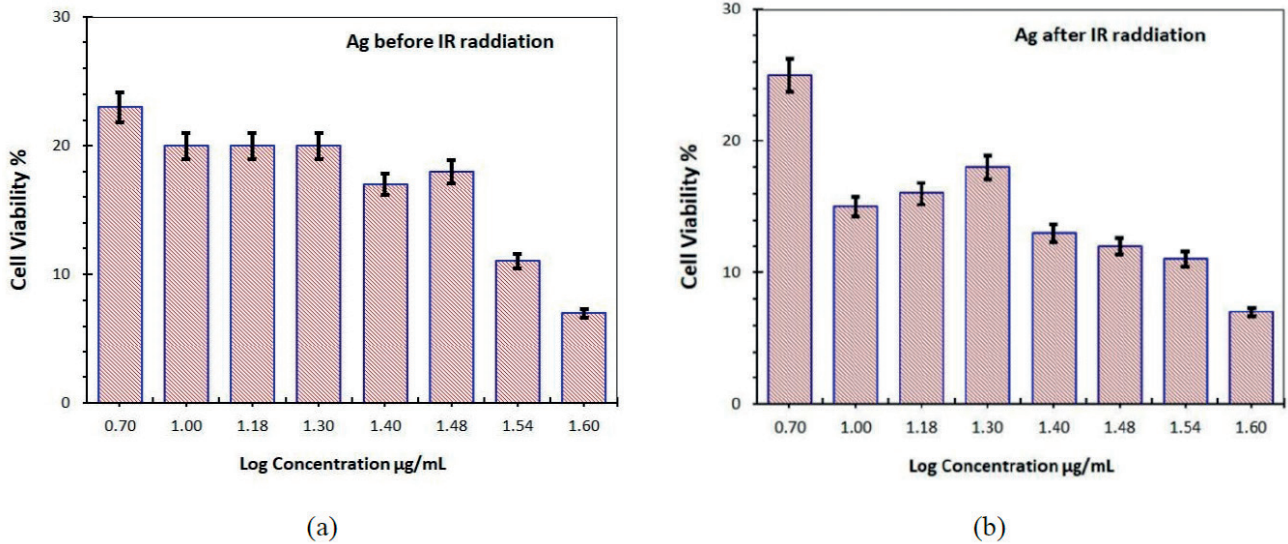


Figure 10. Cell viability of the skin cancer cell treated with Ag NP's (a) without IR radiation (b) with IR radiation.

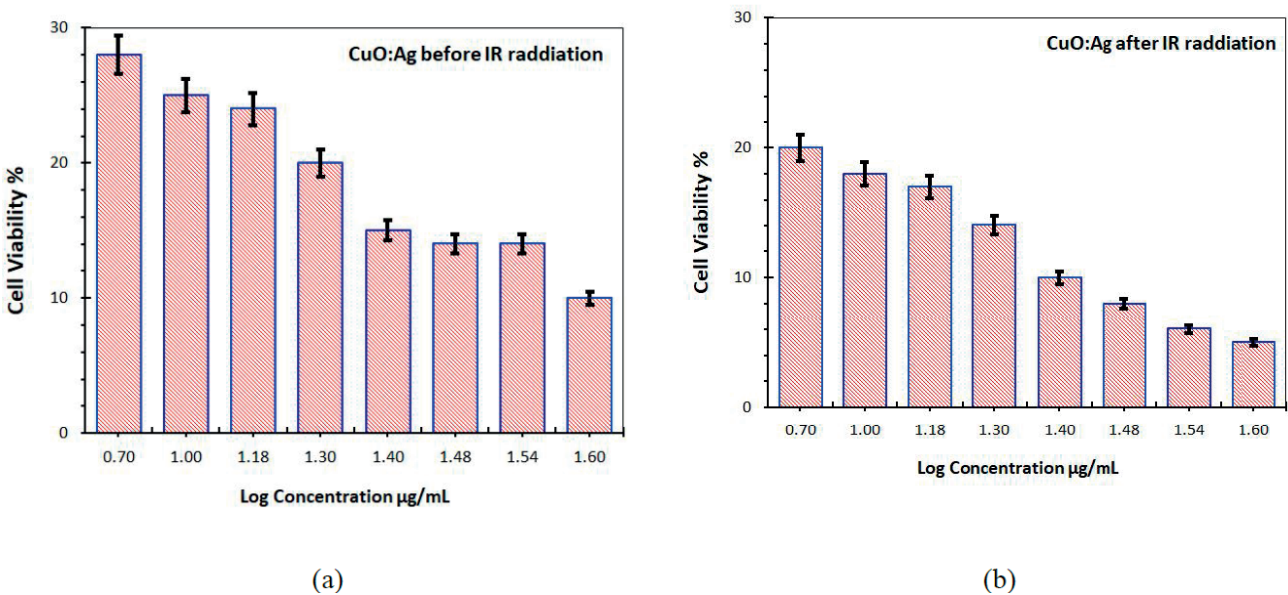


Figure 11. Cell viability of the skin cancer cell treated with CuO:Ag NP's (a) without IR radiation (b) with IR radiation.

cancer cell line significantly decreased as Ag NP's suspension increased with IR exposure. Also, it is clear from Figures (6- b, 7- b and 8- b) that the skin cancer cell line is eliminated by increasing the concentration of CuO NPs suspension to reach the clear image from any cancer cell in Figure (8- a). On the other hand, the skin cancer cell will disappear fast in case of adding a mixing of the two types of synthesized nanoparticles with a mixing ratio (1:1). CuO: Ag NPs are high-efficacy, high-specificity, and low-cost therapy solutions. Dose, exposure period, and the size and form of the Ag NPs all play a role in effective treatment. CuO: Ag NP-mediated apoptosis involves the generation of reactive oxygen species (ROS), mitochondrial membrane rupture, DNA damage, and signaling cascades that lead to programmed cell death. The reference agreed upon this outcome¹⁸. CuO: Ag NPs and skin cancer cells absorbed relatively little yet could be detected through intact and injured skin. However, more excellent permeability has been found in cases of injured skin. Another study, on the other hand, discovered that CuO: Ag NPs could penetrate intact human skin in vivo and could be found beyond the stratum corneum at depths of the reticular dermis. The size of CuO: Ag NPs affects their penetration. AgNPs (20, 50, and 80 nm) were found in the cytoplasmic vacuoles of human epidermal keratinocytes, while CuO: Ag NPs with a diameter of 100 nm were found. Positive controls were utilized to demonstrate that the assay works and to account for the effects of vehicle control. The MTT assay was used to measure cell viability against both cell lines as a positive control. The cancer treatment chosen as positive control is already in use.

Apoptosis and Vacuole degeneration were triggered by Ag NPs, as well as cell formation and the appearance of skin cancer cells. In contrast, the standard cell line (control) showed no phenotypic changes. The Ag NPs had a selective effect in their cytotoxicity, and both induced apoptosis. They could be suggested as a potential therapy because the treatment with Ag NPs increased the expression of a multi-functional tumor suppressor (PTEN) (up to 100-fold more than the control), augmenting the tumor suppressor effects of the PTEN.

Increased levels of reactive oxygen species (ROS) inside cells cause oxidative stress, which leads to cell death via programmed cell death. Furthermore, increasing ROS levels can disrupt mitochondrial membranes, resulting in programmed cell death. Skin cancer cells treated with Ag NPs die due to decreasing glutathione levels and a rise in lipid peroxide levels, which causes the cells to die due to the oxidative stress response. The structure of cellular actin is disrupted by Ag NPs, resulting in cell death. Treatment with Ag NP's can potentially cause mitochondria-dependent apoptosis. Because Ag NPs can dissolve ions, they damage mitochondrial membranes, allowing cytochrome to escape into the cytoplasm. The physical-chemical interaction of biological proteins with the nanoparticles could also cause Ag NPs to affect cancer cells. In the case of IR radiation exposure, cancer cell viability was significantly reduced dose-dependent, as shown in the figure, where viability declined to 60% when the concentration was increased to 100 g/ml (10- b).

In comparison to CuO NPs, adding silver NPs results in poorer cell viability, as shown in the figure, with a percentage cell vitality of 0.2 percent in skin cell lines (11-a). Compared to CuO NPs, Ag NPs have the lowest percentage of cell viability. This could be due to various causes, as evidenced by the fact that Ag NPs do not contain active phytochemi-

cals when mixed with CuO NPs.

When IR radiation was used on these cell lines, the percentage of cell viability of CuO: Ag NPs with a mixing ratio of (1:1) decreased as the concentration increased. Both of these NPs showed decreased percentage cell viability on skin cancer cell lines; however, IR radiation exposure showed minor cell vitality on the cell line at 1.6 g/ml concentration, as shown in Figure 11-b. The results reveal that the longer the skin cell line is exposed to IR radiation in CuO: Ag NPs presence, the lower the cell viability. However, lengthier exposure to normal skin cells has minor harmful effects.

Conclusions

At varying concentrations, copper oxide and silver nanoparticles strongly influenced a skin cancer cell line. Compared to the control, higher concentrations of CuO and Ag NP's resulted in stronger stimulation in cancer cell lines. Even at the lowest dose studied, skin cancer cells appear to be more susceptible. The IR thermogram produced during imaging and IR radiation exposure revealed a link between the nanoparticle concentration obtained from the treatment and the elevated temperature of the treated area. The findings appear to support the use of thermal imaging in treating skin cancer. IR imaging may provide extra insight into a patient's therapy response. When IR radiation was used on these cell lines, the percentage cell viability of CuO:Ag NPs with a mixing ratio of (1:1) decreased as the concentration increased. Moreover on skin cancer cell lines, both of these NPs showed a reduced percentage of cell viability.

Bibliographic references

1. Kapur VK, Redline S, Nieto F, Young TB, Newman AB, Henderson JA.. The relationship between chronically disrupted sleep and healthcare use. *Sleep* 2002; 25(3):289–296.
2. Alves, C., & Rapp, A. Spontaneous abortion (miscarriage). *StatPearls* [Internet]. 2020.
3. Ambühl, L. M. M., Baandrup, U., Dybkær, K., Blaaekær, J., Uldbjerg, N., & Sørensen, S. Human papillomavirus infection as a possible cause of spontaneous abortion and spontaneous preterm delivery. *Infectious diseases in obstetrics and gynecology*, 2016.
4. Betsiol, J., Villa, L. L., & Slichero, L. Impact of HPV infection on the development of head and neck cancer. *Brazilian Journal of Medical and Biological Research*, 2013; 46, 217-226.
5. Bober, L., Guzowski, G., Moczulska, H., & Sieroszewski, P. Influence of human papilloma virus (hPV) infection on early pregnancy. *Ginekologia polska*, 2019; 90(2), 72-75.
6. Bober, L., Guzowski, G., Moczulska, H., & Sieroszewski, P. Influence of human papilloma virus (hPV) infection on early pregnancy. *Ginekologia polska*, 2019; 90(2), 72-75.
7. Bruno, M. T., Caruso, S., Bica, F., Arcidiacono, G., & Boemi, S. Evidence for HPV DNA in the placenta of women who resorted to elective abortion. *BMC pregnancy and childbirth*, 2021; 21(1), 1-6.
8. Burton, G. J., & Watson, A. L. The structure of the human placenta: implications for initiating and defending against virus infections. *Reviews in medical virology*, 1997; 7(4), 219-228.
9. Carabali, M., Austin, N., King, N. B., & Kaufman, J. S. The Zika epidemic and abortion in Latin America: a scoping review. *Global health research and policy*, 2018; 3(1), 1-9.
10. Christiansen, O. B., Elson, J., Kolte, A. M., Lewis, S., Middeldorp, S., Nelen, W., ... & Goddijn, M. (2018). ESHRE guideline: recurrent pregnancy loss. *Human Reproduction Open*, 2018,(2), hoy004-hoy004.

11. Chung, C. H., & Gillison, M. L. Human papillomavirus in head and neck cancer: its role in pathogenesis and clinical implications. *Clinical cancer research*, 2009; 15(22), 6758-6762.
12. Conde-Ferrández, L., May, A. D. A. C., Carrillo-Martínez, J. R., Ayora-Talavera, G., & del Refugio González-Losa, M. Human papillomavirus infection and spontaneous abortion: a case-control study performed in Mexico. *European Journal of Obstetrics & Gynecology and Reproductive Biology*, 2013; 170(2), 468-473.
13. Condrat, C. E., Filip, L., Gherghe, M., Cretoiu, D., & Suci, N. Maternal HPV Infection: Effects on Pregnancy Outcome. *Viruses*, 2021; 13(12), 2455.
14. Cornet, I., Gheit, T., Franceschi, S., Vignat, J., Burk, R. D., Sylla, B. S., ... & IARC HPV Variant Study Group. Human papillomavirus type 16 genetic variants: phylogeny and classification based on E6 and LCR. *Journal of virology*, 2012; 86(12), 6855-6861.
15. Feng, Z. H. Analysis about reason of repeated missed abortion. *J Chin Physician*, 2005; 10, 1382-1383.
16. Galamb, Á., Pethó, B., Fekete, D., Petrányi, G., & Pajor, A. Uterine anomalies in women with recurrent pregnancy loss. *Orvosi hetilap*, 2015; 156(27), 1081-1084.
17. Giakoumelou, S., Wheelhouse, N., Cuschieri, K., Entrican, G., Howie, S. E., & Horne, A. W. The role of infection in miscarriage. *Human reproduction update*, 2016; 22(1), 116-133
18. Guyton, C. and Hall, T. "Text book of medical physiology" .10th ed .W .B. Sanders company . New York. 2006.pp:774-790.